Assessment of spectral UV radiation at Marambio Base, Antarctic Peninsula

Klára Čížková[1,2], Kamil Láska[1], Ladislav Metelka[2], Martin Staněk[2]

[1]Department of Geography, Faculty of Science, Masaryk University, Brno, 611 37, Czech Republic
5   [2]Solar and Ozone Observatory, Czech Hydrometeorological Institute, Hradec Králové, 500 08, Czech Republic

Correspondence to: Klára Čížková (cizkova.klara@mail.muni.cz)

Abstract. This study aims to assess response of spectral UV radiation to different atmospheric and terrestrial factors, including solar zenith angle, ozone, cloud cover and albedo, in southern polar environment. For this purpose, 23260 individual spectra (300–363 nm), obtained by the B199 Mk-III Brewer spectrophotometer at Marambio Base, Antarctic Peninsula Region, over
10   the period 2010–2020, were studied. A neural network model was developed to investigate the effects of the explanatory variables at individual wavelengths. SZA proved to be the most important parameter, followed by cloud cover, TOC, and surface albedo. The relative SZA effect is greatest at the shortest wavelengths, where a 1° decline in SZA results in a 6–18 % increase in UV irradiance (305 nm). Also TOC affects particularly the short wavelengths, while at 305 nm, a 10 DU decrease in TOC causes a 7–13 % increase in UV irradiance. In some seasons (e.g., 2011–2012, 2014–2015, 2018–2019), the large-
15   scale ozone holes caused the UV irradiance at very short wavelengths peak in spring, whereas in other seasons (e.g., 2010–2011, 2012–2013), the maxima at all wavelengths were recorded in summer. The effect of cloud cover was strongest near the fully cloudy sky, and in summer months. Albedo affected the UV irradiance only weakly, its effect was strongest in early spring and late fall.

1 Introduction

20   Solar UV radiation has been a source of scientific interest since its discovery in 1801. The biological effects of UV radiation, such as its erythemal effects in humans, have been first described in the late 19th century, followed by the thorough medical research in the 20th century (Diffey, 1980). Since then, many biological effects have been accounted to UV radiation. Amongst them are, for example, melanin production, skin wrinkling, protein damage, or even the alterations of DNA structure in humans and other organisms, which may lead to melanoma (e.g., Czerwińska and Krzyścin, 2019; Holick, 2016). On the contrary, the
25   exposure to solar UV irradiance catalyzes vitamin D creation, which is essential for musculoskeletal health, and may even lead to the lowering of blood pressure in humans (Young et al., 2021). Of course, the effects of UV irradiance are not only limited to humans and other higher organisms. An increased exposure to UV irradiance may also lead to, for example, the reduction of terrestrial plant productivity, or the inhibition of unicellular organisms, both terrestrial and aquatic (UNEP, 2010).

As stratospheric ozone is the most important gas affecting the absorption of UV radiation in the atmosphere, preventing as much as 97–99 % of incident UV irradiance (e.g., Jovanović et al., 2019, McKenzie et al., 2007), UV radiation research received the greatest attention after the discovery of the Antarctic ozone hole in the 1980s (Chubachi, 1985; Farman et al., 1985). Since then, many events have taken place to eliminate the ozone depletion, most notably the 1987 Montreal Protocol and its numerous amendments (Jovanović et al., 2019). The recent positive stratospheric ozone trends, when for example in September, TOC was reported to grow significantly at rates between 1.8 and 2.8 DU per year (e.g., McKenzie et al., 2019; Pazmiño et al., 2018; Solomon et al., 2016), contributed to a decrease in UV irradiance recorded at various Antarctic sites (Bernhard and Stierle, 2020). However, ozone hole still keeps forming each Antarctic spring, increasing the UV irradiances and threatening the rare Antarctic ecosystems (e.g., Cordero et al., 2022). UV radiation assessment is, therefore, still an important scientific task in both hemispheres, including for example the Arctic ozone loss in spring 2020 (e.g., Bognar et al., 2021).

The solar UV spectrum is commonly divided into three bands: UVC (200–290 nm), which is almost entirely absorbed in the atmosphere, UVB (290–320 nm), and UVA (320–400 nm), which is the least photobiologically active. However, this division is semi-arbitrary, and there is no clear transition between UVA and UVB bands, as it is illustrated even by the possible division at 315 nm (Diffey, 1990; Juzeniene et al., 2011). Despite this rather simple division, the precise shape of the solar UV spectrum is far more complex. It is given mostly by the incident solar irradiance at the top of the atmosphere and the wavelength-dependent absorption of UV irradiance by various atmospheric gases (e.g., Kerr and Fioletov, 2008). The extraterrestrial solar spectrum has long been described, and the strong absorption at certain wavelengths has been explained by the Fraunhofer lines, for example the strong Fe line at about 358 nm or the NH line at 336 nm (Stair, 1951). The major atmospheric absorbers in the UVB region are ozone, nitrogen dioxide and sulfur dioxide, but due to their respective abundance, ozone reduces the surface UV irradiance 200 to 300 times more than the other two (DeLuisi, 1997). The UVB region is mostly affected by the Huggins absorption band, which spreads between approximately 310 and 370 nm and exhibits a sequence of wave-like structures (Qu et al., 2004).

Spectral UV observations require a quality instrument with high sensitivity, satisfactory wavelength resolution and precise stray light rejection (Webb, 1991). Such instruments only became available in the 1990s. Since then, the solar UV spectra have been monitored at various locations already for several decades (e.g., McKenzie et al., 1993; Webb, 1991), especially after the introduction of the double monochromator Brewer Mk-III spectrophotometer (Bais, 1997). However, the assessment of spectral solar UV irradiance in the Antarctic remains quite rare, especially without further processing. In most studies from Antarctica, UV irradiance is integrated using various action spectra, most commonly the UV Index or the erythemal action spectrum, or several selected wavelengths or their intervals are evaluated. So far, the entire solar UV spectrum has been mentioned only in few instances, such as the case studies from Union Glacier Camp by Cordero et al. (2014) or Escudero Station by Cordero et al. (2013). However, the above-mentioned studies only included short observation campaigns, so a complex evaluation of long time series of solar UV irradiance spectra from Antarctica is still missing.

2

This study aims to contribute to closing this gap by assessing the 10 year long time series of spectral UV irradiances recorded at Marambio Base in the Antarctic Peninsula region. We focused on UV climatology and year to year differences, extreme values, as well as on the factors affecting the UV irradiance at individual wavelengths. We studied the effects of solar zenith
65   angle (SZA), total ozone column (TOC), cloud cover and albedo using artificial neural network modelling (ANN), which allowed us to focus on key factor and linkages between the southern polar vortex and UV irradiance reaching the Antarctic continent. The paper is organized in two main sections: Section 2 gives the data and methods used in the study, while the study site is specified in Section 2.1, the instrumentation used for solar UV spectral irradiance observation in Section 2.2, and other datasets (SZA, TOC, cloud cover and albedo) are described in Section 2.3. Further on, Section 2.4 states the methods used for
70   data processing and analyses, including the ANN model and its validation. Section 3 then gives the results of this study and also compares them in a wider context, while Section 3.1 focuses on the climatology and changes of spectral UV irradiance and the selected explanatory variables, and Section 3.2 presents the effects of the explanatory variables on the spectral UV irradiance as computed through the ANN model. Lastly, Section 4 summarizes the main findings.

2 Materials and Methods

75   ### 2.1 Study Site

The measurements assessed in this study took place at Marambio Base (S 64.14°, E 56.37°, 196 m a. s. l.). This permanent Argentinean base was founded in 1969 and it is located on the ice-free Seymour Island in the Antarctic Peninsula region. The mean temperature doesn't exceed 0°C in any month, so snow cover, which increases UV radiation reflection, may be present all year long. The cloudiest season is summer, with fog being prevalent especially in December and January (Lakkala et al.,
80   2018; 2020). Marambio Base lies close to the edge of the southern polar vortex (Fig. 1), so during its existence in Antarctic winter and spring, the station lies just inside (about 60 %), on the edge, or just outside the vortex (Karhu et al., 2003; Pazmiño et al., 2005).

2.2 Solar UV Spectra

The solar UV spectra have been obtained by the B199 double monochromator Brewer spectrophotometer over the period from
85   February 2010 to January 2020. During this time, the B199 spectrophotometer was operated by the Czech Hydrometeorological Institute and the National Meteorological Service of Argentina. The instrument was serviced each year in January or February by specialists from the Czech Hydrometeorological Institute and International Ozone Services, Inc., Canada. Moreover, in 2012 and 2016, the B199 spectrophotometer was calibrated against the world traveling standard B017 directly at Marambio Base.

90   The B199 spectrophotometer obtains the spectral UV irradiance within the interval 286.5–363.0 nm, where the bandwidth is 0.5 nm. However, the very short wavelengths present higher uncertainty due to pronounced atmospheric attenuation and the sensitivity of the instrument itself (Bais, 1997; Bojkov et al., 1995). Moreover, the shortest wavelengths are also strongly

absorbed by ozone, which leads to a very weak transmitted information affected by noise and the dark signal of the detector, and an uncertainty exceeding 10 % (Cordero et al., 2008; 2016). Therefore, only the wavelengths longer than 300 nm were

95   used in this study.

Over the period of its operation, the B199 spectrophotometer obtained 45 073 solar UV spectra, each of which was quality-checked for spikes, and the wavelength shift was analyzed based on Fraunhofer lines. The 23 260 of the spectra, which had been successfully paired with explanatory variables (see Section 2.3), were used for this study. The temporal distribution of the spectra is shown in Fig. 2. It can be seen there were several data gaps, of which the longest occurred due to a remotely

100   discovered technical failure of the instrument at the end of 2016. This mechanical problem was resolved early in 2017 during the regular maintenance so the measurements could continue.

2.3 Explanatory Variables

Each of the solar UV spectra used in this study has been paired with following explanatory variables: solar zenith angle (SZA), measured during each of the B199 spectral observations, total ozone column (TOC), cloud cover, and albedo. According to

105   Petkov et al., 2016, these belong to the most important variables affecting UV irradiance at the nearby Mendel Station.

The TOC values used in this study have also been acquired by the B199 Brewer spectrophotometer. Due to their very high precision, which can reach up to 0.15 % (Scarnato et al., 2010), only the Direct Sun measurements have been taken in account. The solar UV spectra have been paired with these independent TOC observations, while only the TOC values within 60 minutes from the spectral measurements have been used. Therefore, more solar spectra could be matched with the same TOC

110   measurement, provided it was taken within the 60 minute time distance and it was the closest observation. When there was no match of the spectrum with a Direct Sun TOC measurement within the specified time interval, the spectrum was removed from the dataset. The 60 minute interval was chosen as a compromise between retaining a large solar UV spectra dataset and precision of the match with TOC. Due to the rapidly changing position of the polar vortex, the TOC values can vary greatly even within a relatively short time period. For example, a case study from the south Argentinean city Rio Gallegos by Orte et

115   al. (2019) showed a drop in TOC by 70 DU in 24 hours, and Nichol and Valenti (1993) state that at South Pole, TOC may vary by more than 20 DU within several hours.

In order to express the effect of cloudiness, the ERA5 reanalysis data (Hersbach et al., 2020) were used. The spatial resolution was 0.25° × 0.25°, and the temporal resolution 1 hour. This dataset was chosen due to the best correlation (r = 0.26) with the Marambio Base cloud modification factor (CMF, Park et al., 2017). CMF was calculated from the ground based UV irradiance

120   data from B199, and the theoretical clear-sky UV irradiance was estimated using the one dimensional DISORT solver of the libRadtran radiative transfer package (Mayer and Kylling, 2005). The CMF itself could not be paired with the UV spectra, as it was not independent of the studied variable.

The albedo values for the Marambio Base location have been taken from the OMI surface UV algorithm (OMUVB) product of the NASA's Aura Ozone Monitoring Instrument, which provides surface albedo at 360 nm (Tanskanen et al., 2006). The

125 spatial resolution is 13 × 24 km at nadir, and only observation with less than 1 hour time difference from the individual spectra were included.

2.4 Data Processing and Analysis

The data analyses were carried out for the solar spectra, as well as for the explanatory variables (SZA, TOC, cloudiness, albedo). At first, basic statistical characteristics were calculated for the entire period, individual months and seasons. Due to

130 the non-normal distribution of the datasets, median was chosen as the preferred measure of central tendency, alongside with the use of nonparametric testing where applicable (e.g., Mann-Whitney U test and Kruskal-Wallis ANOVA, described in Kruskal and Wallis, 1952). All tests were performed at the significance level $\alpha = 0.05$.

In order to assess the change of UV irradiance over the study period, daily median spectra have been calculated, as well as their relative differences to the 2010–2020 median. The solar irradiances at 305 and 340 nm have been further emphasized.

135 These wavelengths have been chosen because of their different absorption by ozone (Bernhard and Stierle, 2020), but also because the results could be easily compared with other studies (e.g., Bernhard et al., 2005, 2006; Diaz et al., 2006; or Stamnes et al., 1991). At these wavelengths, the distribution of very high values was studied as well. A very high value was defined as belonging in the top 10 % of all measured irradiances at the given wavelength.

The climatological effects of explanatory variables (SZA, TOC, cloudiness, and albedo) were assessed using an artificial

140 dataset built by an ANN model (see further in this section). Such model was preferred to a parametric multiple regression model because according to DeVaux et al., 1993, ANN models are suitable for noisy or intercorrelated (Table 1) input data and to express nonlinear relationships.

Ten different ANN multilayer perceptron models were built, each with four inputs (SZA, TOC, cloudiness, and albedo) and 127 outputs (UV irradiance at the studied wavelengths in the interval 300.0–363.0 nm, with 0.5 nm resolution). Each time, the

145 dataset was randomly divided into a training subset (70 % of the data), testing subset (15 %), and validation subset (15 %). At the beginning of the training, each network was randomly initialized with a normal distribution with mean = 0 and standard deviation = 1. The stopping condition was set to the error improvement lower than 0.0000001 in the window of 200 cycles, while the error function was defined as the sum of squares.

Using the validation dataset, the performance of all ten models was assessed, and the best one was selected based on the

150 absolute and relative bias, root mean square error (RMSE), and correlation with the original data. According to the sensitivity analysis, SZA was the most important variable in the selected model, with the weight of 4.54, followed by cloud cover (1.14), TOC (1.05), and surface albedo (1.00).

However, even in the best of the ten models, a systematic bias was observed. So a correction was carried on: median bias values were calculated from the entire dataset separately for each wavelength and month, and then they were subtracted from

155 the model output. The correction for medians tackled the systematic underestimation of UV irradiance at almost all wavelengths (Fig. 3a,b). After the correction, 80 % of the data fitted between ±0.08 mW·m^{-2}. The relative differences were greater at very short wavelengths, but from approximately 310 nm, 80 % of the data did not exceed approximately ±25 %,

which can also be seen in Fig. 3c. The correction improved the amount of data within ±1, 5, 10, and 25 %, in average by 0.5, 1.6, 2.0, and 1.5 %, respectively. The observations shared between 76 and 92 % of variability (Fig. 3d), while R-squared was

160   greater at shorter wavelengths. The correction for medians increased the shared variability in average by 0.1 %. RMSE was greater at longer wavelengths, and after the correction, it changed only within approximately ±0.0001 mW·m^{-2}.

After the best model was selected and the correction was performed, the effect of explanatory variables on the UV spectra was estimated. Out of the four explanatory variables, always just a single one was left to its original value, while the three other variables were fixed to their monthly medians (Table 2). The use of individual months' medians was applied because neural

165   networks generally present good results within the scope of the dataset, but they are not ideal for extrapolation, as they tend to overfit to the training dataset (e.g., Raksasat et al., 2021). So, modelling UV irradiance outside the dataset range, e.g., at a low SZA and very low TOC, could lead to very imprecise results. The breakdown of the dataset into individual months and the use of monthly medians prevented these inaccuracies, so it was possible to calculate the UV irradiance change attributed to each of the four studied variables in the nine individual months.

170   Based on the above-described modelled data, the linearity and strength of the relationships were studied. At first, the relationships for each month at 305 and 340 nm were plotted, and then the mean absolute and relative change in spectral UV irradiance induced by the explanatory variables was assessed. The final part of the analysis consisted of several case studies, where the modelled values were compared to the actual observed spectra. Each time, two spectra, one with a very high and the other with a very low value of a particular explanatory variable, were chosen, and the observed and modelled spectra were

175   compared. Due to the difference of monthly median and the actual values, the differences between the model and the observation showed also the combined effect of the other explanatory variables.

3 Results and Discussion

3.1 Solar UV spectra climatology and changes

Median solar UV irradiance generally increases with increasing wavelength. The increase is faster in the UVB region, up to

180   ~330 nm (Fig. 4a), where it makes in average 0.007 mW·m^{-2}·nm^{-1} but the shape is approximately exponential. At longer wavelengths, the increase changes to quasi-linear and slows down to 0.002 mW·m^{-2}·nm^{-1}. This behavior is well represented in all months but due to the respective position of the Sun and the studied site, it is steeper in low-SZA months (Fig. 4b). At shorter wavelengths (up to approx. 330 nm), the increase in median irradiance varies from 0.003 mW·m^{-2}·nm^{-1} in April to 0.010 mW·m^{-2}·nm^{-1} in December and January. At longer wavelengths, the irradiance variability increase is smaller and makes

185   0.001 mW·m^{-2}·nm^{-1} in August, September, March and April, and 0.002 mW·m^{-2}·nm^{-1} in other months. The precise shape of the spectrum, given by the extraterrestrial irradiance and atmospheric attenuation, remains similar in all months, with a higher variability between local maxima and minima in spring and autumn (effect of low SZA).

The relative differences of monthly medians to the overall median vary especially at wavelengths to about 320 nm (Fig. 4c). At 300 nm, the UV irradiance exceeds the overall median by up to 139 % in January and reaches only 7 % of it in April.

190   However, at 363 nm, the monthly medians make up between 135 and 52 % of the overall one, so the difference is smaller. The change of the relative differences gradient in months affected by the ozone hole may be possibly attributed to the effect of variable ozone amount. In October, when the UV irradiance is lower than the overall median, the difference decreases with decreasing wavelengths, while in November, when the median irradiance already exceeds the overall median, the difference increases more steeply. The wave-like Huggins belt structure, visible in certain months, is likely also conditioned by the amount

195   of ozone relative to the general central tendency (e.g., Gorshelev et al., 2014).

TOC (Fig. 4d) exhibits a pattern typical for Antarctic environment, i.e. depletion in austral spring, explained for example in Karhu et al. (2003) or Koo et al. (2018). In September, the median TOC value drops below the 220 DU level, while the absolute minimum, 113.7 DU, was recorded on 3 November 2015. In November and December, the median TOC values grow above the summer medians, which is likely due to the advection of subpolar, ozone rich air masses into the area of the decaying polar

200   vortex. Over the study period, the highest TOC value was recorded on 6 November 2011, when it reached 402.0 DU.

The large variability of cloud cover at Marambio Base, with the median value of 68 % and mean of 59 %, is expressed in Fig. 4e. For the latitude of Marambio, Lachlan-Cope (2010) presents a higher mean cloud cover (around 80 %). This difference is likely due to the position of Marambio at the eastern, i.e. leeward side of the Antarctic Peninsula. There is a hint of weak yearly cycle with maxima in September and minima in February, but the differences between the months are not statistically

205   significant. In the Antarctic Peninsula region, both Adhikari et al. (2012), Lachlan-Cope (2010) and Scott et al. (2017) found the cloud cover minima in winter and maxima in summer. However, due to the large cloud cover variability, mentioned also in Aun et al. (2020), the results presented in this study might have been affected by the choice of study period.

Median surface albedo at Marambio Base fluctuates between 0.42 in January and 0.61 in August (Fig. 4f). Due to the snow melting and sea ice reduction, albedo decreases in the summer season, but in March the sea ice recovers and albedo increases.

210   Even though the differences between individual months are statistically significant, albedo can occasionally approach 0.8 even in summer months. This is likely related to snowfall events, because at the Antarctic Peninsula, most precipitation falls in solid form, even though in summer, liquid precipitation can occur too (e.g., Ambrožová et al., 2020; Carrasco and Cordero, 2020).

The spectral UV irradiance represented in Fig. 5a shows a clear year to year variability with minima in early spring and late autumn and maxima in Antarctic summer. However, the attenuation of UV irradiance in the atmosphere, caused likely by the

215   action of clouds and atmospheric gases, frequently disrupts the dominant pattern. The lower intensity at some wavelengths (e.g., 316.5 nm or 358.5 nm), which is in Fig. 5a represented by the relatively darker vertical lines, has been caused by the presence of Fraunhofer absorption lines.

Although the absolute variability of UV irradiance is highest at the longer wavelengths, the relative variability (Fig. 5b) is greatest at the shortest wavelengths, as seen from the presence of highest and lowest values of the ratio between the daily

220   median spectra and the overall median (in Fig. 5b, it is expressed on logarithmic scale). Also here, the minima occur in early spring and late autumn, but the maxima can be recorded both in summer and spring. This is further documented by Fig. 5c and 5e, which implies that at 305 nm, solar UV irradiance maxima can occur in October, as well as in December or January. For example, in the seasons 2010–2011 or 2017–2018 the summer (January) maximum, caused likely by low cloud cover, is more

pronounced. However, in other seasons, such as in 2011–2012, 2014–2015 or 2018–2019, UV irradiance at 305 nm peaks in

225 spring, particularly in October and November. The spring peak is affected mostly by ozone, which attenuates especially radiation of very short wavelengths (e.g., Bais et al., 1993; Gorshelev et al. 2014). Very short wavelengths seem to follow a similar pattern with a large, ozone-induced variability in spring at different locations in Antarctica, such as McMurdo Station (Bernhard et al., 2006), or Palmer Station (Bernhard et al., 2005), but also in the southernmost South America (Diaz et al., 2006). On the contrary, at 340 nm (Fig. 5d), the summer maximum is higher in all cases except the 2014–2015 season. This

230 wavelength is considered largely unaffected by ozone, however, despite being affected much less than shorter wavelengths, in the cases of some deep ozone holes (e.g., seasons 2013–2014, which was short-lasting but deep and correlated with a drop in cloud cover, or 2018–2019, where a decrease in cloud cover was also observed), irradiance increases can be seen even at longer wavelengths.

Alongside atmospheric gases, the surface UV irradiance is also affected by the absorption in the troposphere, which is in this

235 study represented by the cloud cover. As seen from Table 2 and Fig. 4e, during the study period, maxima tend to occur in spring and minima in early fall, but there is much year to year variability (Fig. 5f). Near the Antarctic Peninsula, cloudiness can attenuate more than 90 % of UV irradiance, but in the case of a thin cloud cover and a short optical path through the atmosphere, this number can shrink to as little as 30 % (Lee et al., 2015). However, this amount is likely not the same at all wavelengths, as due to the increased scattering of shorter wavelengths in the atmosphere and thus the decreasing proportion

240 of direct radiation (described e.g., in Schwander et al., 2002), clouds affect solar radiation at longer wavelengths more. Nevertheless, it seems that during cloudy days, such as in September 2010 or August to October 2017, UV irradiances at Marambio drop at both short and long wavelengths, while below-median cloudiness (e.g., December 2015) caused high summer UV irradiance peaks.

Surface properties, represented by albedo, were found to be another important factor affecting the spectral UV irradiance.

245 Snow or sea ice can reflect 50 to 95 % of UV radiation, depending on SZA and surface quality, such as soot content. However, the ocean without sea ice only reflects 5–20 % of UV radiation, which may lead to its decline compared to snow cover or glaciated areas (Cordero et al., 2014; Zhou et al., 2019). Around Marambio Base, albedo reaches maxima at the end of winter (August to October), and minima in late summer (January to February). This annual variation is quite steady with only little deviations from the climatological median (Fig. 5g), caused likely by snowfall events or, on the other hand, excessive snowmelt

250 in the vicinity of Marambio Base.

Very high UV irradiances at Marambio Base at 305 and 340 nm were identified especially in spring and summer, typically from October to February (Fig. 6). Due to the effect of low ozone values, UV irradiance at 305 nm often peaks earlier than at 340 nm, and there are large differences between the number of high UV irradiances at 305 and 340 nm in each month. The two datasets only share less than 52 % of variability, what proves that it is important to study UV irradiance at separate

255 wavelengths individually. For example, in October 2010, there were no high UV irradiances at 340 nm, but there were 34 of them at 305 nm. Although the ozone reduction in 2010 was relatively small (Fig. 5e, de Laat and van Weele, 2011), relatively low cloudiness (median of 43 %, as seen in Fig. 5f) allowed the UV irradiance at 305 nm to reach very high values. Similarly,

in the season 2011–2012, there were 12 cases of very high UV irradiances at 305 nm already in September and 84 of them in October, while there were only 3 cases at 340 nm in October 2011. In 2011, the ozone hole was relatively severe (Fig. 5e,

260   Klekociuk et al., 2014), so it strongly affected the UV irradiance at 305 nm. Another similar example, where relatively deep and stable polar vortex with low ozone content increased the number of very high irradiance measurements at 305 nm but not at 340 nm, was the season 2018–2019 (Fig. 5e, and e.g., Klekociuk et al., 2021). On the contrary, in November 2017, only 18 cases of high UV irradiances were recorded at 305 nm, compared to 113 cases at 340 nm. This was due to very high TOC in November 2011 (the median value of TOC was 357.4 DU), which attenuated the solar irradiance at 305 nm.

265   ### 3.2 Effects of explanatory variables on spectral UV irradiance

As seen from Fig. 7–10, the relationships between UV irradiance and explanatory variables, as modelled by the ANN model described in Section 2.4, are often not linear, and vary based on wavelength. The relationships and amounts of change for different months also vary, which demonstrates that they are affected by other variables. Therefore, Fig. 7–10 show examples of the relationships of the explanatory variables and UV irradiance, given that all other variables are fixed to their monthly

270   medians.

Out of the four studied variables, SZA is the most important one affecting the UV irradiance at Marambio Base (Fig. 7). The relationship between UV irradiance and SZA at 305 nm (Fig. 7a) is not linear, as the increase in UV irradiance at lower SZA is faster than at high SZA values. Compared to other months, UV irradiance at 305 nm in September and October increases faster with the decrease in SZA, which is likely caused by its enhancements by the low TOC values in the ozone-hole period.

275   The relationship between SZA and the modelled UV irradiance is getting rather linear with increasing wavelength (Fig. 7b), and the relative differences between individual months are smaller. The nonlinearity of the relationship can be explained by the solar UV irradiance being indirectly proportional to the cosine of SZA, and by the increasing absorption and scattering in the atmosphere as the optical path lengthens (e.g., Kerr and Fioletov, 2008). The absolute mean differences in UV irradiance for the 1° increase in SZA are greater at wavelengths longer than about 320 nm (Fig. 7c), but the relative changes are largest

280   at the very short wavelengths (Fig. 7d). For example, at 340 nm, a 1° increase in SZA causes between 3 % decline in UV irradiance in December and 8 % in August, but at 305 nm, this change varies between 6 % in December and 18 % in March, provided all other variables are fixed to their monthly medians. Webb and Engelsen (2008) explain this by the increasing path of UV radiation through the ozonosphere, so the short wavelengths are attenuated more than the longer ones. The spectral dependence of the relationship between UV irradiance and SZA has also been shown in the case studies by Kerr and Fioletov

285   (2008) or Tarasick et al. (2003), and indirectly also by the 340/305 nm ratio studied by Stamnes et al. (1991).

The fact that ozone affects UV irradiance more at shorter wavelengths can also be seen from Fig. 8. UV irradiance at 305 nm increases with the decrease in TOC (Fig. 8a) at an average rate of up to 0.002 mW·m^{-2} per 10 DU in November, but the relationship is nonlinear, with a faster increase at low TOC values. A similar, approximately exponential relationship of TOC and UV irradiance at 300 nm from South Argentina has been presented by Bojkov et al. (1995). The differences in the

290   relationships between the studied months are likely caused by the effect of SZA, as also Kerr at al. (2008) observed a much

steeper decline in UV irradiance at 300 nm in low-SZA conditions. At 340 nm, TOC is only weak absorber of UV radiation (e.g., Gorshelev et al., 2014), so it does not have a profound effect at this wavelength (Fig. 8b). Nevertheless, in the low-SZA months, UV irradiance increases by up to 0.004 mW·m^{-2} in January with a 10DU decrease in ozone, though the relationship is nonlinear. The rather complex shape of the relationship is likely to be an artifact of the ANN model. The mean absolute change

295   in UV irradiance induced by a 10DU increase in TOC is greatest at about 317.5 nm, ranging from -0.004 mW·m^{-2} in August to -0.006 mW·m^{-2} in January (Fig. 8c). On the contrary, the relative change is greatest at the shortest wavelengths, and it is getting close to 0 at the longer ones (Fig. 8d; also described in Bais et al., 1993). The Huggins belt wavy structure is clearly visible between approximately 315 and 335 nm.

According to the ANN model, the effect of cloudiness (Fig. 9) seems to be generally quite weak at both 305 and 340 nm (Fig.

300   9a,b), being greater near the fully cloudy sky. The absolute change in spectral UV irradiance caused by a 10 % increase in cloud cover is greatest at the longer wavelengths (Fig. 9c), but the relative change is largest at the shortest wavelengths, especially in high-SZA months (Fig. 9d). However, from about 313 nm, the relative change of modelled UV irradiance remains almost the same, and it ranges from about -0.2 % in April to approximately -2.2 % in January. Although Bais et al. (1993) did not find any spectral dependence of the relationship between UV irradiance and cloud cover, Seckmeyer et al. (1996) and

305   Kylling at al. (1997) argue that due to spectrally dependent Rayleigh scattering of UV radiation at top of cloud layer, the cloud transmittance is higher at shorter wavelengths. Similarly, Schwander et al. (2002) found that in the UVA region, the attenuation of UV radiation by clouds increases with increasing wavelength. The clouds can attenuate up to 99 % of UV radiation, however, their effect is generally weaker over the Antarctic continent, possibly explaining the relatively small changes detected by the modelling experiment. This happens because the Antarctic clouds are thinner than the ones in middle and low latitudes,

310   affecting the portion of UV radiation penetrating through them (Calbó et al., 2005; Lubin and Frederick, 1991). Also Lee et al. (2015) show that in the Antarctic Peninsula region, the increase in cloud cover from clear sky to overcast causes only about 30 % decrease in erythemal UV irradiance, and this change is even smaller at high SZA. Similarly to this study, they show a nonlinear relationship with a faster decline in erythemal UV irradiance when the cloud cover exceeds approximately 5 octas.

The last variable affecting UV irradiance, which is covered in this study, is surface albedo (Fig. 10). The relationship between

315   albedo and UV irradiance is almost linear, although weak at both 305 and 340 nm (Fig. 10a,b). Generally, UV irradiance decreases with a decreasing albedo (Fig. 10c,d), while at wavelengths longer than 320 nm, a 0.1 change in albedo results in up to 1.5% increase in UV irradiance (in April). However, in other months, such as November, December and January, the albedo effect is not significant. According to the results of this study, at 320 nm, the change in albedo from 0.1 to 0.9 can lead to up to 26% increase in UV irradiance (in April). The change is greater in high-SZA months, which is in concordance with Lee et

320   al. (2015). Cordero et al. (2014) state that albedo greater than 90 % can increase UV irradiance by up to 50 %, and Lee at al. (2015) say that the relative increase in UV irradiance on snow covered surfaces ranges between 15–30 %. However, since the albedo of different surfaces, including snow, is spectrally dependent (Wuttke et al., 2006) and the satellite data used in this study cover relatively large surface areas, the relationships described here can be seen as climatological, large-scale ones.

Looking at individual case studies featuring a solar spectrum measured at a high SZA and a solar spectrum measured at a low
325   SZA (Fig. 11a), the modelled values confirm the relative increase or decrease of UV irradiance is greatest at the shortest
wavelengths. However, this is not the case in the selected low-SZA measurement, as the short wavelengths are attenuated by
a very high ozone content (about 120 DU higher than the monthly median, to which the model run was set). Therefore, the
effect of SZA can be at least partly overrun by the effects of other explanatory variables, as seen from the contrast of the model
and observation. The two case studies presented in Fig. 11b show measurements with the record-high and record-low October
330   TOC, differing from each other by as much as 274 DU. The modelled UV irradiances are very close to the October median at
wavelengths longer than about 320 nm, but at shorter wavelengths, the model irradiances deviate from each other. This shows
that even at extremely low TOC conditions, the UV irradiance may not be record high due to other factors (e.g., SZA,
cloudiness). Therefore, the mismatch between the observed and modelled low-TOC irradiances can be explained by the effect
of SZA, which was in reality more than 15° higher than the monthly median, which was used in the model. The modelled
335   values presented in Fig. 11c show a minor difference between the 0 % and 100 % cloud cover, which is almost independent of
the wavelength. Similarly as in the previous cases, the ground based observations differ from the model due to the effect of
explanatory variables, most likely SZA. In the case of albedo, there is almost no difference between the modelled UV
irradiances in the high and low albedo case (Fig. 11d), stating that the large-scale albedo as recorded by the satellites is the
least important variable of the four covered by this study. The observations differ from the models based on SZA, TOC, or
340   even cloudiness, and due to the combination of these variables, the high-albedo case exhibits lower UV irradiances than the
low-albedo case. However, in the long-term, albedo changes may become a more important factor affecting UV irradiance
even on the regional scale. The Antarctic sea ice extent, which is the most important variable for the large-scale Antarctic
Peninsula region albedo, is recently hitting record lows (e.g., Turner et al., 2022), so late summer to early fall UV irradiances
may decrease. The absorbed solar radiation may then contribute to the sea ice – albedo positive feedback, causing even larger
345   sea ice loss, with all its climatological consequences.

4 Summary and Conclusion

UV radiation is an important factor affecting the life on Earth, but its effects are spectrally dependent. However, in the southern
polar areas, a detailed analysis of solar UV spectra and their response to different atmospheric and terrestrial factors was still
missing. In this study a comprehensive analysis of spectral UV radiation, based on 10 years of Brewer spectrophotometer
350   measurements, was carried out using the approach of neural network modelling. It helped to confirm the strongly wavelength-
dependent behavior of UV irradiance, showing the importance of spectral UV radiation assessment. The absolute differences
between the UV irradiance spectra generally increase with increasing wavelength, but the relative differences are greater at
the shortest wavelengths. In the studied months (August to April) at Marambio Base, the highest median UV irradiance was
recorded in January (139 % of the overall median at 300 nm, 135 % at 363 nm), whereas the lowest one in April (7 % of the
355   overall median at 300 nm, 52 % at 363 nm). However, in some seasons (e.g., 2011–2012, 2014–2015, 2018–2019), UV

11

irradiance at the shortest studied wavelengths peaked in spring (October and November). The temporal distributions of very high UV irradiances at 305 and 340 nm only share less than 52 % of variability, showing that UV irradiances at different parts of the spectrum respond differently to the driving factors, such as SZA, TOC, cloud cover or surface albedo.

SZA is the most important variable affecting UV irradiance at Marambio Base. According to the ANN model, the increase in
360 UV irradiance with the decrease in SZA is faster at short wavelengths, when at 305 nm, a 1° decline in SZA equals between 6 and 18 % increase in UV irradiance, but only between 3 and 8 % at 340 nm, depending on the month. At Marambio Base, TOC shows a pattern typical for the southern polar conditions with a pronounced depletion in spring. Over the 2010–2020 period, the spring depletion was variable, with deep, long-lasting ozone holes in the seasons 2011–2012 or 2015–2016. The absolute TOC minimum was reached on 3 November 2015. On the other hand, the 2019 ozone hole was the smallest on record.

365 In seasons with a deep, long-lasting ozone hole, the spring peak of the UV irradiances at very short wavelengths is most visible. The relationship between TOC and UV irradiance at 305 nm is non-linear, with a faster increase at low TOC values. At this wavelength, a 10 DU increase in TOC causes between 7 and 13 % decrease in UV irradiance. At 340 nm, TOC does not have a profound effect.

Due to the relatively thin Antarctic clouds, the effect of cloud cover on UV irradiance was found rather weak. The increase in
370 cloud cover by 10 % caused between 1–2 % decrease in UV irradiance at both 305 and 340 nm, while the attenuation increased fastest between 90 % and 100 % cloudiness. Also the effect of satellite-based surface albedo was assessed as relatively weak, when a 0.1 increase in albedo represented only up to 2 % increase in UV irradiance at 320 nm and more.

Additional efforts are needed to extend this study by the evaluation of other variables, such as on-site snow cover or the sea ice area in a given perimeter around Marambio Base, because the albedo of different surfaces, including snow, is spectrally
375 dependent. Similarly, cloud type may also be studied, as it is also an important variable affecting UV irradiance. Also it is important to note that the results of this study might have been influenced by the peculiar characteristics of the given location, so they cannot be easily applied to the entire Antarctic Peninsula region.

Data availability

The solar radiation data used for the study are property of the Czech Hydrometeorological Institute, Hradec Králové, Czech
380 Republic and are the subject of the data policy of the above-mentioned institution. Any person interested in the underlying data should contact Ladislav Metelka, the head of the Solar and Ozone Observatory of the Czech Hydrometeorological Institute, Hradec Králové (email: metelka@chmi.cz). The satellite and reanalyzed data courtesy of NASA and ECMWF, respectively.

Author contribution

385 K.Č., K.L. and L.M. designed the study, L.M. and M.S. provided the resources, L.M. and M.S. designed the ANN model and K.Č. validated it, K.Č. performed the data analyses and prepared the original manuscript draft, while K.L. and L.M. reviewed and edited it.

Competing interests

The authors declare that they have no conflict of interest.

390 **Special issue statement**

The work was presented online at the Quadrennial Ozone Symposium 2021 (poster No. SAT3_9) and we have expressed the interest to submit the paper to the joint Special Issue "Atmospheric ozone and related species in the early 2020s: latest results and trends" in ACP/AMT journals following on the QOS2021.

References

Adhikari, L., Wang, Z., and Deng, M.: Seasonal variations of Antarctic clouds observed by CloudSat and CALIPSO
405 satellites, J. Geophys. Res., 117 (D04202), 1–17, 2012, DOI: 10.1029/2011JD016719.
Ambrožová, K., Hrbáček, F., and Láska, K.: The Summer Surface Energy Budget of the Ice-Free Area of Northern James Ross Island and Its Impact on the Ground Thermal Regime, Atmosphere-Basel, 11 (877), 1–18, 2020, DOI: 10.3390/atmos11080877.

Arola, A., Lakkala, K., Bais, A., Kaurola, J., Meleti, C., and Taalas, P.: Factors affecting short- and long-term changes of
410   spectral UV irradiance at two European stations, J. Geophys. Res., 108 (D17), 1–9, 2003, DOI: 10.1029/2003JD003447.

Aun, M., Lakkala, K., Sanchez, R., Asmi, E., Nollas, F., Meinander, O., Sogacheva, L., De Bock, V., de Leeuw, G.,
Aaltonen, V., Bolsée, D., Cizkova, K., Mangold, A., Metelka, L., Jakobsen, E., Svendby, T., Gillotay, D., and Van Opstal,
B.: Solar UV radiation measurements in Marambio, Antarctica, during years 2017–2019, Atmos. Chem. Phys., 20, 6037–
6054, 2020.

415   Bais, A.: Absolute spectral measurements of direct solar ultraviolet irradiance with a Brewer spectrophotometer, Appl.
Optics, 36, 5199–5204, 1997.

Bais, A., Zerefos, C. S., Meleti, C., Ziomas, I. C., and Tourpali, K.: Spectral Measurements of Solar UVB Radiation and
its Relations to Total Ozone, SO2, and Clouds, J. Geophys. Res., 98 (D3), 5199–5204, 1993.

Bernhard, G.: Trends of solar ultraviolet irradiance at Barrow, Alaska, and the effect of measurement uncertainties on
420   trend detection, Atmos. Chem. Phys., 11, 13029–13045, 2011.

Bernhard, G., Booth, C., Ehramjian, J. C.: UV climatology at Palmer Station, Antarctica, based on Version 2 NSF network
data, Proc. SPIE, 5886, 1–12, 2005, DOI: 10.1117/12.614172.

Bernhard, G., Booth, C. R., Ehramjian, J. C., and Nichol, S. E.: UV climatology at McMurdo Station, Antarctica, based
on version 2 data of the National Science Foundation's Ultraviolet Radiation Monitoring Network, J. Geophys. Res., 111
425   (D11201), 1–15, 2006, DOI: 10.1029/2005JD005857.

Bernhard, G., and Stierle, S.: Trends of UV Radiation in Antarctica, Atmosphere-Basel, 11 (795), 1–26, 2020, DOI:
10.3390/atmos11080795.

Bognar, K., Ramina, A., Strong, K., Chipperfield, M. P., Dhomse, S. S., Drummond, J. R., Feng, W., Fioletov, V., Goutail,
F., Herrera, B., Manney, G. L., McCullough, E. M., Millán, L. F., Pazmiño, A., Walker, K. A., Wizenberg, T., and Zhao,
430   X.: Unprecedented Spring 2020 Ozone Depletion in the Context of 20 Years of Measurements at Eureka, Canada, J.
Geophys. Res.-Atm., 126 (8), 2021, DOI: 10.1029/2020JD034365.

Bojkov, R. D., Fioletov, V. E., and Diaz, S. B.: The relationship between solar UV irradiance and total ozone from
observations over southern Argentina, Geophys. Res. Lett., 22, 1249–1252, 1995.

Calbó, J., Pagès, D., and Gonzáles, J.-A.: Empirical studies of cloud effects on UV radiation: a review, Rev. Geophys., 43
435   (RG2002), 1–28, 2005, DOI: 10.1029/2004RG000155.

Carrasco, J. F. and Cordero, R. R.: Analyzing Precipitation Changes in the Northern Tip of the Antarctic Peninsula during
the 1970–2019 Period, Atmosphere-Basel, 11 (1270), 1–19, 2020, DOI: 10.3390/atmos11121270.

Chubachi, S.: A Special Ozone Observation at Syowa Station, Antarctica from February 1982 to January 1983. In: Zerefos
C.S., Ghazi A. (eds) Atmospheric Ozone. Springer, Dordrecht, 285–289, DOI: 10.1007/978-94-009-5313-0_58.

440   Cordero, R. R., Seckmeyer, G., Pissulla, D., DaSilva, L., and Labbe, F.: Uncertainty evaluation of spectral UV irradiance
measurements, Meas. Sci. Technol., 19 (045104), 1–15, 2008, DOI: 10.1088/0957-0233/19/4/045104.

14

Cordero, R. R., Damiani, A., Seckmeyer, G., Riechelmann, S., Labbe, F., Laroze, D., and Garate, F.: Satellite-derived UV climatology at Escudero Station, Antarctic Peninsula, Antarct. Sci., 25, 731–803, 2013.

Cordero, R. R., Damiani, A., Ferrer, J., Jorquera, J., Tobar, M., Labbe, F., Carrasco, J, and Laroze, D.: UV Irradiance and
445   Albedo at Union Glacier Camp (Antarctica): A Case Study, PLOS ONE, 9 (e90705), 1–9, 2014, DOI: 10.1371/journal.pone.0090705.

Cordero, R. R., Damiani, A., Seckmeyer, G., Jorquera, J., Caballero, M., Rowe, P., Ferrer, J., Mubarak, R., Carrasco, J., Rondanelli, R., Matus, M., and Laroze, D.: The Solar Spectrum in the Atacama Desert, Sci. Rep.-UK, 6 (22457), 1–15, 2016, DOI: 10.1038/srep22457.

450   Cordero, R. R., Feron, S., Damiani, A., Redondas, A., Carrasco, J., Sepúlveda, E., Jorquera, J., Fernandoy, F., Llanillo, P., Rowe, P. M., and Seckmeyer, G.: Persistent extreme ultraviolet irradiance in Antarctica despite the ozone recovery onset, Sci. Rep.-UK, 12, 1–10, 2022, DOI: 10.1038/s41598-022-05449-8.

Czerwińska, A. and Krzyścin, J. W.: Climatological aspects of the increase of the skin cancer (melanoma) incidence rate in Europe, Int. J. Climatol., 40, 3196–3207, 2019.

455   De Laat, A. T. J., and Van Weele, M.: The 2010 Antarctic ozone hole: Observed reduction in ozone destruction by minor sudden stratospheric warmings, Sci. Rep.-UK, 1 (38), 1–8, 2011, DOI: 10.1038/srep00038.

DeLuisi, J.: Atmospheric Ultraviolet Radiation Scattering and Absorption, NATO ASI Ser., 52, 65–84, 1997.

De Vaux, R. D., Psichogios, D. C., and Ungar, L. H.: A Comparison of Two Nonparametric Estimation Schemes: MARS and Neural Networks, Comput. Chem. Eng., 17, 819–837, 1993.

460   Diaz, S., Camilión, C., Deferrari, G., Fuenzalida, H., Armstrong, R., Booth, C., Paladini, A., Cabrera, S., Casicca, C., Lovengreen, C., Pedroni, J., Rosales, A., Zagarese, H., and Vernet, M.: Ozone and UV Radiation over Southern South America: Climatology and Anomalies, Photochem. Photobiol., 82, 834–843, 2006.

Diffey, B. L.: Ultraviolet radiation physics and the skin, Phys. Med. Biol., 25, 405–426, 1980.

Diffey, B. L.: Solar ultraviolet radiation effects on biological systems, Phys. Med. Biol., 36, 299–328, 1990.

465   Durbin, J., and Watson, G. S.: Testing for serial correlation in least squares regression I, Biometrika, 37, 409–428, 1950.

Farman, J. C., Gardiner, B. G., and Shanklin, J. D.: Large losses of total ozone in Antarctica reveal seasonal ClOx/NOx interaction, Nature, 315, 207–210, 1985.

Fitzka, M., Simic, S., and Hadzimustafic, J.: Long-term trends in spectral surface UV irradiance at Hoher Sonnblick (3106 m a.s.l.), AIP Conf. Proc., 1531, 776–779, 2013.

470   Glandorf, M., Arola, A., Bais, A., and Seckmeyer, G.: Possibilities to detect trends in spectral UV irradiance, Theor. Appl. Climatol., 81, 33–44, 2005.

Gorshelev, V., Serdyuchenko, A., Weber, M., Chehade, W., and Burrows, J. P.: High spectral resolution ozone absorption cross-sections – Part 1: Measurements, data analysis and comparison with previous measurements around 293 K, Atmos. Meas. Tech., 7, 609–624, 2014.

475   Hersbach, H., Bell, B., Berrisford, P., Hirahara, S., Horányi, A., Muñoz-Sabater, J., Nicolas, J., Peubey, C., Radu, R., Schepers, D., Simmons, A., Soci, C., Abdalla, S., Abellan, X., Balsamo, G., Bechtold, P., Biavati, G., Bidlot, J., Bonavita, M., De Chiara, G., Dahlgren, P., Dee, D., Diamantakis, M., Dragani, R., Flemming, J., Forbes, R., Fuentes, M., Geer, A., Haimberger, L., Healy, S., Hogan, R. J., Hólm, E., Janisková, M., Keeley, S., Laloyaux, P., Lopez, P., Lupu, C., Radnoti, G., de Rosnay, P., Rozum, I., Vamborg, F., Villaume, S., and Tépaut, J.-N.: The ERA5 global reanalysis, Q. J. Roy.

480   Meteor. Soc., 146, 1999–2049, 2020.

Holick, M. F.: Biological Effects of Sunlight, Ultraviolet Radiation, Visible Light, Infrared Radiation and Vitamin D for Helath, Anticancer Res., 36, 1345–1356, 2016.

Jovanović, Đ., Lukinović, M., and Vitošević, Z.: Environment and health – thirty years of successful implementation of the Montreal Protocol, Srp. Ark. Celok. Lek., 147, 492–496, 2019.

485   Juzeniene, A., Brekke, P., Dahlback, A., Andersson-Engels, S., Reichrath, J., Moan, K., Holick, M. F., Grant, W. B., and Moan, J.: Solar radiation and human health, Rep. Prog. Phys., 74, 1–56, 2011, DOI: 10.1088/0034-4885/74/6/066701.

Karhu, J. A., Taalas, P., Damski, J., and Kaurola, J.: Vertical distribution of ozone at Marambio, Antarctic Peninsula, during 1987–1999, J. Geophys. Res., 108 (D17, 4545), 1–9, 2003, DOI: 10.1029/2003JD001435.

Kerr, J. B. and Fioletov, V. E.: Surface Ultraviolet Radiation, Atmos. Ocean, 46, 159–184, 2008.

490   Klekociuk, A. R., Tully, M. B., Krummel, P. B., Gies, H. P., Petelina, S. V., Alexander, S. P., Deschamps, L. L., Fraser, P. J., Henderson, S. I., Javorniczky, J., Shanklin, J. D., Siddaway, J. M., and Stone, K. A.: The Antarctic ozone hole during 2011, Aust. Meteorol. Ocean., 64, 293–311, 2014.

Klekociuk, A. R., Tully, M. B., Krummel, P. B., Henderson, S. I., Smale, D., Querel, R., Nichol, S., Alexander, S. P., Fraser, P. J., and Nedoluha, G.: The Antarctic ozone hole during 2018 and 2019, J. South. Hemisphere Earth Syst. Sci.,

495   71, 66–91, 2021.

Koo, J.-H., Choi, T., Lee, H., Kim, J., Ahn, D. H., Kim, J., Kim, Y.-H., Yoo, C., Hong, H., Moon, K.-J., and Lee, Y. G.: Total ozone characteristics associated with regional meteorology in West Antarctica, Atmos. Environ., 195, 78–88, 2018.

Kruskal, W. H., and Wallis, W. A.: Use of Ranks in One-Criterion Variance Analysis, J. Am. Stat. Assoc., 47, 583–621, 1952.

500   Kylling, A., Albold, A., and Seckmeyer, G.: Transmittance of a cloud is wavelength-dependent in the UV-range: Physical interpretation, Geophys. Res. Lett., 24, 397–400, 1997.

Lachlan-Cope, T.: Antarctic clouds, Polar Res., 29, 150–158, 2010.

Lakkala, K., Redondas, A., Meinander, O., Thölix, L., Hamari, B., Almansa, A.F., Carreno, V., García, R. D., Torres, C., Deferrari, G., Ochoa, H., Bernhard, G., Sanchez, R. and de Leeuw, G.: UV measurements at Marambio and Ushuaia

505   during 2000–2010, Atmos. Chem. Phys., 18, 16019–16031, 2018.

Lakkala, K., Aun, M., Sanchez, R., Bernhard, G., Asmi, E., Meinander, O., Nollas, F., Hülsen, G., Aaltonen, V., Arola, A, and de Leeuw, G.: New continuous total ozone, UV, VIS and PAR measurements at Marambio, 64°S, Antarctica, Earth Syst. Sci. Data, 12, 947–960, 2020.

16

510   Lee, Y. G., Koo, J.-H., and Kim, J.: Influence of cloud fraction and snow cover to the variation of surface UV radiation at King Sejong station, Antarctica, Atmos. Res., 164–165, 99–109, 2015.

Lubin, D. and Frederick, J. E.: The Ultraviolet Environment of the Antarctic Peninsula: The Roles of Ozone and Cloud Cover, J. Appl. Meteorol., 30, 478–493, 1991.

Mayer, B. and Kylling, A.: Technical note: The libRadtran software package for radiative transfer calculations – description and examples of use, Atmos. Chem. Phys., 5, 1855–1877, 2005.

515   McKenzie, R., Kotkamp, M., Seckmeyer, G., Erb, R., Roy, C. R., Gies, H. P., and Toomey, S. J.: First Southern Hemisphere Intercomparison of Measured Solar UV Spectra, Geophys. Res. Lett., 20, 2223–2226, 1993.

McKenzie, R., Aucamp, P. J., Bais, A. F., Björn, L. O., and Ilyas, M.: Changes in biologically-active ultraviolet radiation reaching the Earth's surface, Photochem. Photobiol. Sci., 2007, 218–231, 2007.

McKenzie, R., Bernhard, G., Liley, B., Disterhoft, P., Rhodes, S., Bais, A., Morgenstern, O., Newman, P., Oman, L.,
520   Brogniez, C., and Simic, S.: Success of Montreal Protocol Demonstrated by Comparing High-Quality UV Measurements with "World Avoided" Calculations from Two Chemistry-Climate Models, Sci. Rep.-UK, 9, 1–13, 2019, DOI.: 10.1038/s41598-019-48625-z.

Nichol, S. E. and Valenti, C.: Intercomparison of total ozone measured at low sun angles by the Brewer and Dobson spectrophotometers at Scott Base, Antarctica, Geophys. Res. Let., 20, 2051–2054, 1993.

525   Orte, P. F., Wolfram, E., Salvador, J., Mizuno, A., Bègue, N., Bencherif, H., Bali, J. L., D'Elia, R., Pazmiño, A., Godin-Beekmann, S., Ohyama, H., and Quiroga, J.: Analysis of a southern sub-polar short-term ozone variation event using a millimeter-wave radiometer, Ann. Geophys., 37, 613–629, 2019.

Park, S. S., Kim, M., Lee, H., Lee, H., Kim, S.-M., and Lee, Y. G..: Estimating Cloud and Aerosol UV Modification Factors Based on Spectral Measurement from the Brewer Spectrophotometer, Atmosphere-Basel, 8 (109), 1–17, 2017,
530   DOI: 10.3390/atmos8060109.

Pazmiño, A., Godin-Beekmann, S., Ginzburk, M., Bekki, S., Hauchecorne, A., Piacentini, R. D., and Quel, E. J.: Impact of Antarctic polar vortex occurrences on total ozone and UVB radiation at southern Argentinean and Antarctic stations during 1997–2003 period, J. Geophys. Res., 110 (D03103), 1–13, 2005, DOI: 10.1029/2004JD005304.

Pazmiño, A., Godin-Beekman, S., Hauchecorne, A., Claud, C., Khaykin, S., Goutail, F., Wolfram, E., Salvador, J., and
535   Quel, E.: Multiple symptoms of total ozone recovery inside the Antarctic vortex during Austral spring, Atmos. Chem. Phys., 18, 7557–7572, 2018.

Petkov, B. H., Láska, K., Vitale, V., Lanconelli, C., Lupi, A., Mazzola, M., and Budíková, M.: Variability in solar irradiance observed at two contrasting Antarctic sites, Atmos. Res., 172–173, 126–135, 2016.

Qu, Z.-W., Zhu, H., Grebenshchikov, S. Y., Schinke, R., and Farantos, S. C.: The Huggins band of ozone: A theoretical
540   analysis, J. Chem. Phys., 121, 11731–11745, 2004.

Raksasat, R., Sri-iesaranusorn, P., Pemcharoen, J., Laiwarin, P., Buntoung, S., Janjai, S., Boontaveeyuwat, E., Asawanonda, P., Sriswasdi, S., and Chuangsuwanich, E.: Accurate surface ultraviolet radiation forecasting for clinical applications with deep neural network, Sci. Rep.-UK, 11 (5031), 1–12, 2021, DOI: 1038/s41598-021-84396-2.

545   Scarnato, B., Staehlin, J., Stübl, R, and Schill, H.: Long-term total ozone observations at Arosa (Switzerland) with Dobson and Brewer instruments (1988–2007), J. Geophys. Res., 115 (D13306), 1–11, 2010, DOI: 10.1029/2009JD011908.

Schwander, H., Koepke, P., Kaifel, A., and Seckmeyer, G.: Modification of spectral UV irradiance by clouds, J. Geophys. Res., 107 (D16), 1–12, 2002, DOI: 10.1029/2001JD001297.

Scott, R., Lubin, D., Vogelman, A. M., and Kato, S.: West Antarctic Ice Sheet Cloud Cover and Surface Radiation Budget from NASA A-Train Satellites, J. Climate, 30, 6151–6170, 2017.

550   Seckmeyer, G., Erb, R., and Albold, A.: Transmitance of a cloud is wavelength-dependent in the UV-range, Geophys. Res. Lett., 23, 2753–2755, 1996.

Solomon, S., Ivy, D. J., Kinnison, D., Mills, M. J., Neely, R. R., and Schmidt, A.: Emergence of healing in the Antarctic ozone layer, Science, 353, 269–274, 2016.

Stair, R.: Ultraviolet Spectral Distribution of Radiant Energy From the Sun, J. Res. Nat. Bur. Stand., 46, 353–357.

555   Stamnes, K., Slusser, J., and Bowen, M.: Derivation of total ozone abundance and cloud effects from spectral irradiance measurements, Appl. Optics, 30, 4418–4426, 1991.

Tanskanen, A., Krotkov, N. A., Herman, J. R., and Arola, A.: Surface Ultraviolet Irradiance from OMI, IEEE T. Geosci. Remote, 44, 1267–1271 , 2006.

Tarasick, D. W., Fioletov, V. E., Wardle, D. I., Kerr, J. B., McArthur, L. J. B., and McLinden, C. A.: Climatology and trends of surface UV radiation, Atmos. Ocean, 41, 121–138, 2003.

560   Turner, J., Holmes, C., Harrison, T. C., Phillips, T., Jena, B., Reeves-Francois, T., Fogt, R., Thomas, E. R., and Bajish, C. C.: Record Low Antarctic Sea Ice Cover in February 2022, Geophys. Res. Lett., 49 (12), 1–11, 2022, DOI: 10.1029/2022GL098904.

UNEP: Environmental effects of ozone depletion and its interaction with climate change: 2010 assessment, United Nations
565   Environment Programme (UNEP), Nairobi, 278, 2010.

Webb, A. R.: Ultraviolet radiation: the missing link in the ozone debate, Norsk Geol. Tidsskr., 71, 211–213, 1991.

Webb, A. R. and Engelsen, O.: Ultraviolet Exposure Scenarios: Risks of Erythema from Recommendations on Cutaneous Vitamin D Synthesis, Adv. Exp. Med. Biol., 624, 72–85, 2008.

Wuttke, S., Seckmeyer, G., and König-Langlo, G.: Measurements of spectral snow albedo at Neumayer, Antarctica, Ann.
570   Geophys., 24, 7–21, 2006.

Young, A. R., Morgan, K. A., Harrison, G. I., Lawrence, K. P., Petersen, B., Wulf, H. C., and Philipsen, P. A.: A revised action spectrum for vitamin D synthesis by suberythemal UV radiation exposure in humans in vivo, PNAS, 118 (e2015867118), 1–8, 2021, DOI: 10.1073/pnas.2015867118.

Zhou, C., Zhang, T., and Zheng, L.: The Characteristics of Surface Albedo Change Trends over the Antarctic Sea Ice

575   Region during Recent Decades, Remote Sens.-Basel, 11 (821), 1–25, 2019, DOI: 10.3390/rs11070821.

Table 1: Intercorrelation of explanatory variables (SZA = solar zenith angle; TOC = total ozone column; CLD = cloudiness; ALB = albedo). Statistically significant results (α = 0.05) are marked with an asterisk.

|	SZA	TOC	CLD
TOC	-0.23*	·	·
CLD	-0.04*	-0.12*	·
ALB	0.20*	-0.19*	-0.01

580

Table 2: Monthly median values of explanatory variables (SZA = solar zenith angle; TOC = total ozone column; CLD = cloudiness; ALB = albedo) at Marambio Base in 2010–2020, which were used to fix the variables in the ANN model runs.

|	AUG	SEP	OCT	NOV	DEC	JAN	FEB	MAR	APR
SZA	76.11	70.13	61.75	55.60	52.12	53.50	59.27	67.12	74.59
TOC	246.5	205.5	223.7	300.2	311.4	287.8	283.7	273.6	283.0
CLD	67	76	73	70	66	64	62	67	71
ALB	0.61	0.60	0.62	0.57	0.47	0.42	0.43	0.51	0.59
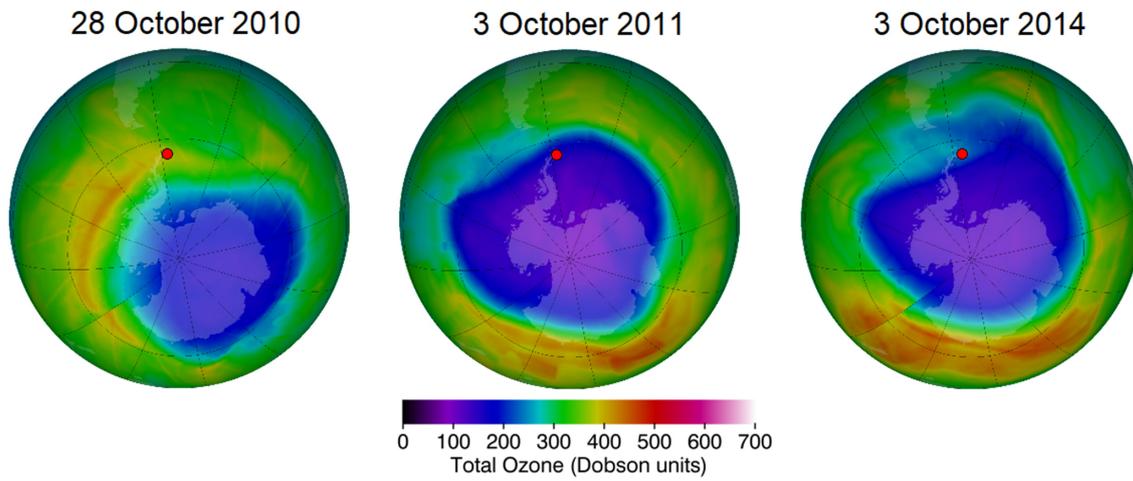
585

Figure 1: The approximate position of Marambio Base (red dot) relative to the southern polar vortex (outside, inside, and on the edge) on different October days. Image adapted from Ozone Hole Watch (2022).
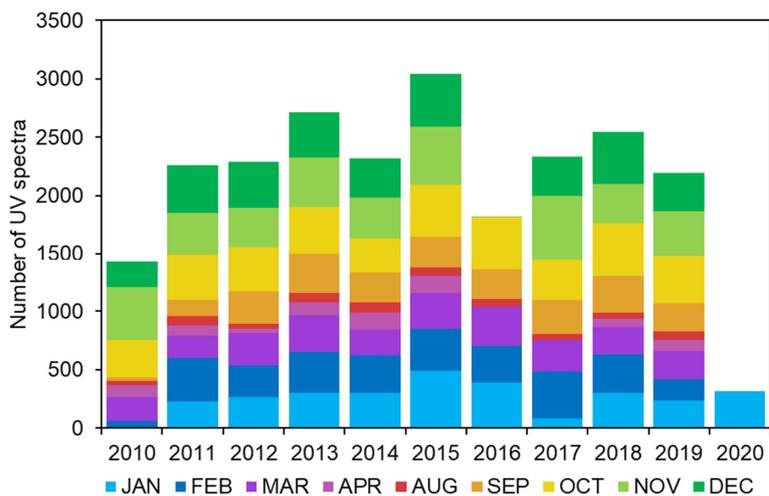
Figure 2: Number of solar UV spectra used in this study measured by the B199 Brewer spectrophotometer at Marambio Base over the period 2010–2020.
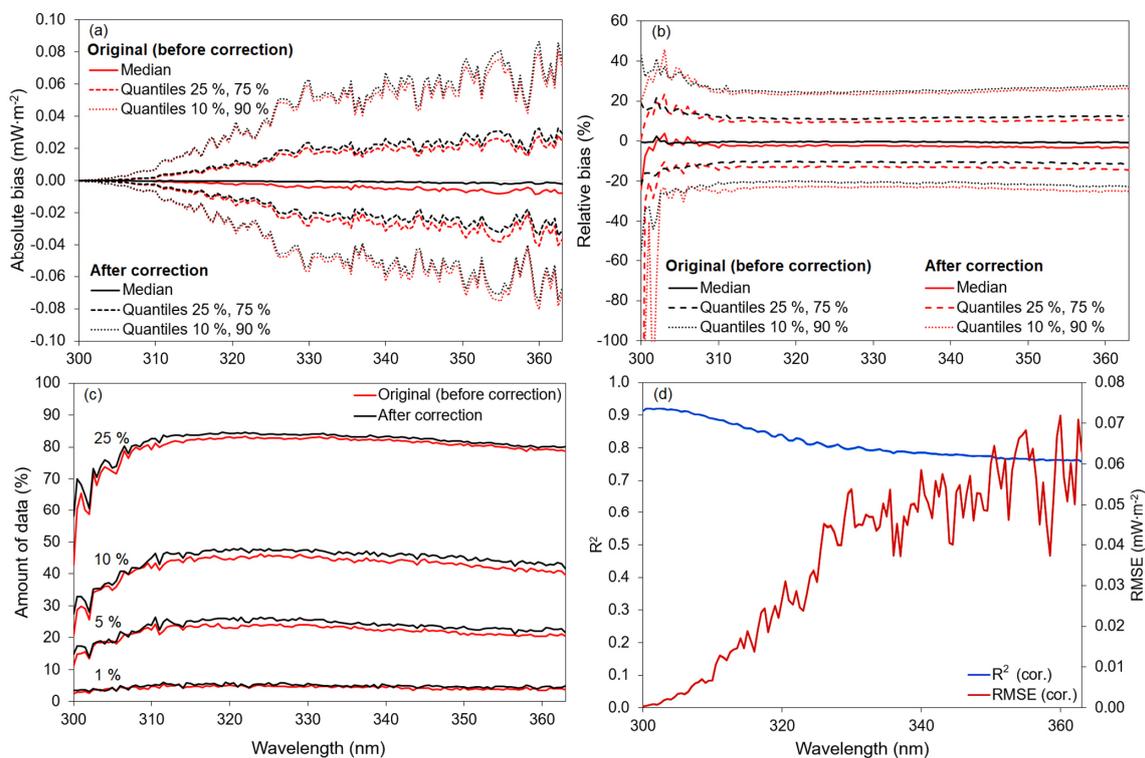
Figure 3: Validation of the ANN model before and after the median correction, while (a) represents the absolute bias quantiles, (b) are the relative bias quantiles, (c) is the amount of data within 1, 5, 10, and 25 % from observations, and (d) is the R-squared and RMSE.
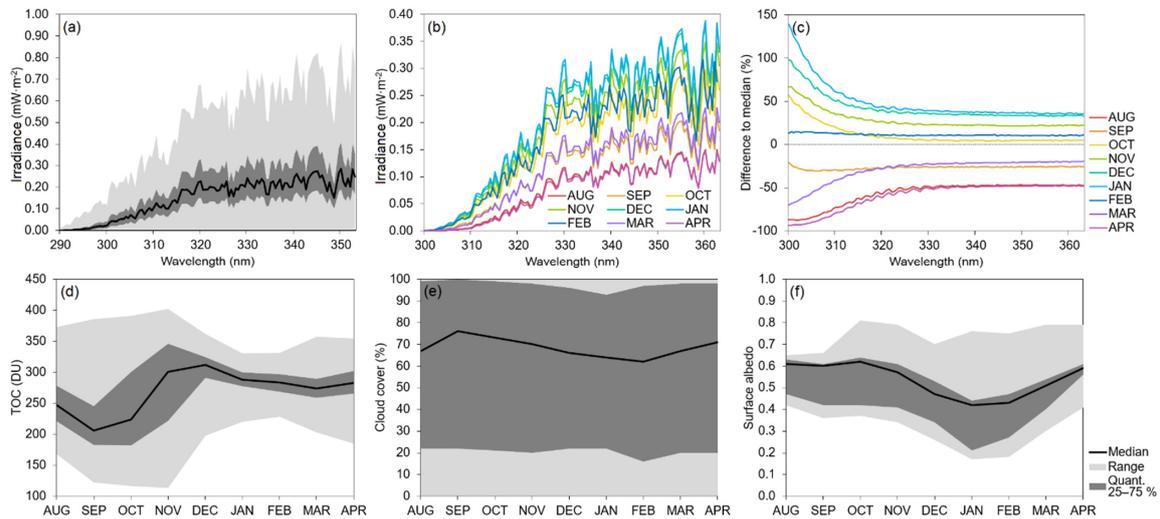
Figure 4: Observed solar UV spectra and variables related to them obtained at Marambio Base in 2010–2020, while (a) represents statistical characteristics of all spectra, (b) monthly medians, and (c) relative differences of monthly medians to overall median, and (d), (e) and (f) show the climatology of TOC, cloud cover, and surface albedo, respectively.

600
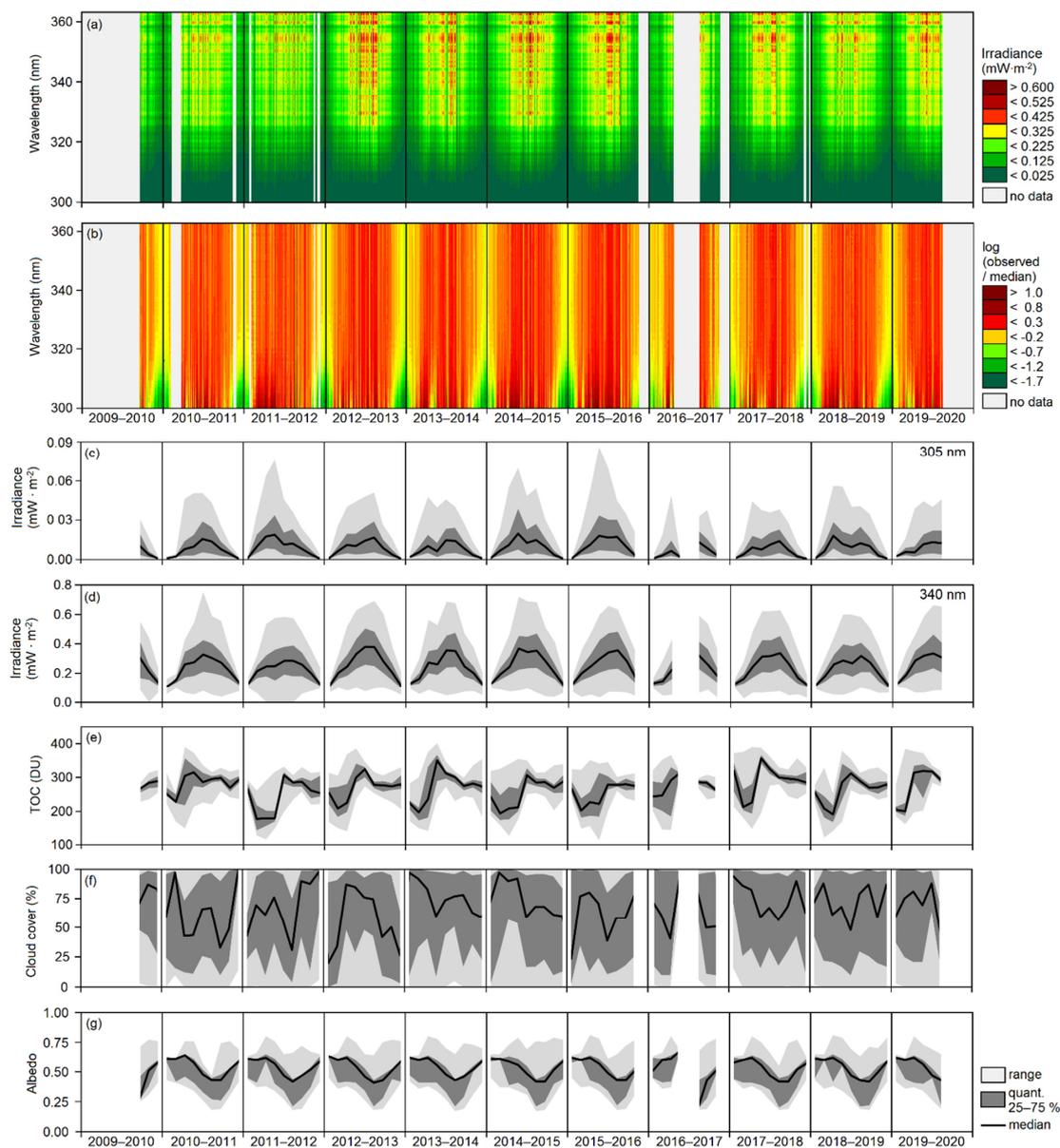
Figure 5: UV irradiance and related variables at Marambio Base over the period 2010–2020, while (a) represents the daily median intensities of spectral UV irradiance, (b) the daily median spectral UV irradiances relative to the overall median, on logarithmic scale, at a given wavelength, (c) the monthly variability of solar irradiance at 305 nm, (d) the monthly variability of solar irradiance at 340 nm, (e) the monthly variability of TOC, (f) the monthly variability of cloud cover, and (g) the monthly variability of albedo.

605
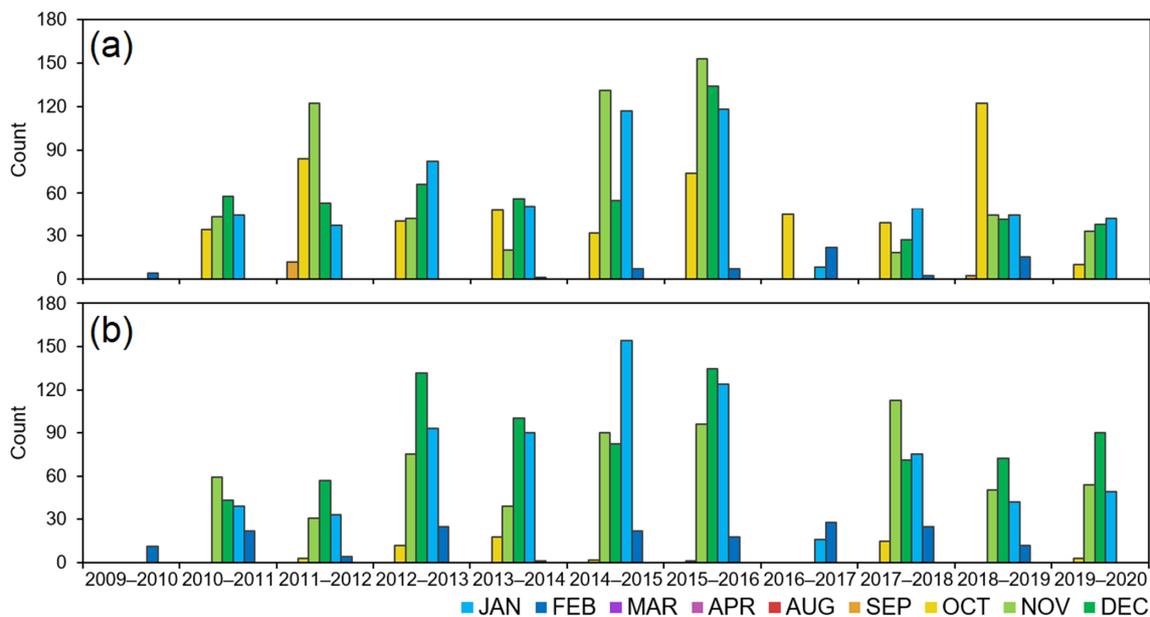
Figure 6: Monthly distribution of the 10 % highest UV irradiances at (a) 305 nm, and (b) 340 nm, at Marambio Base, 2010–2020.

610
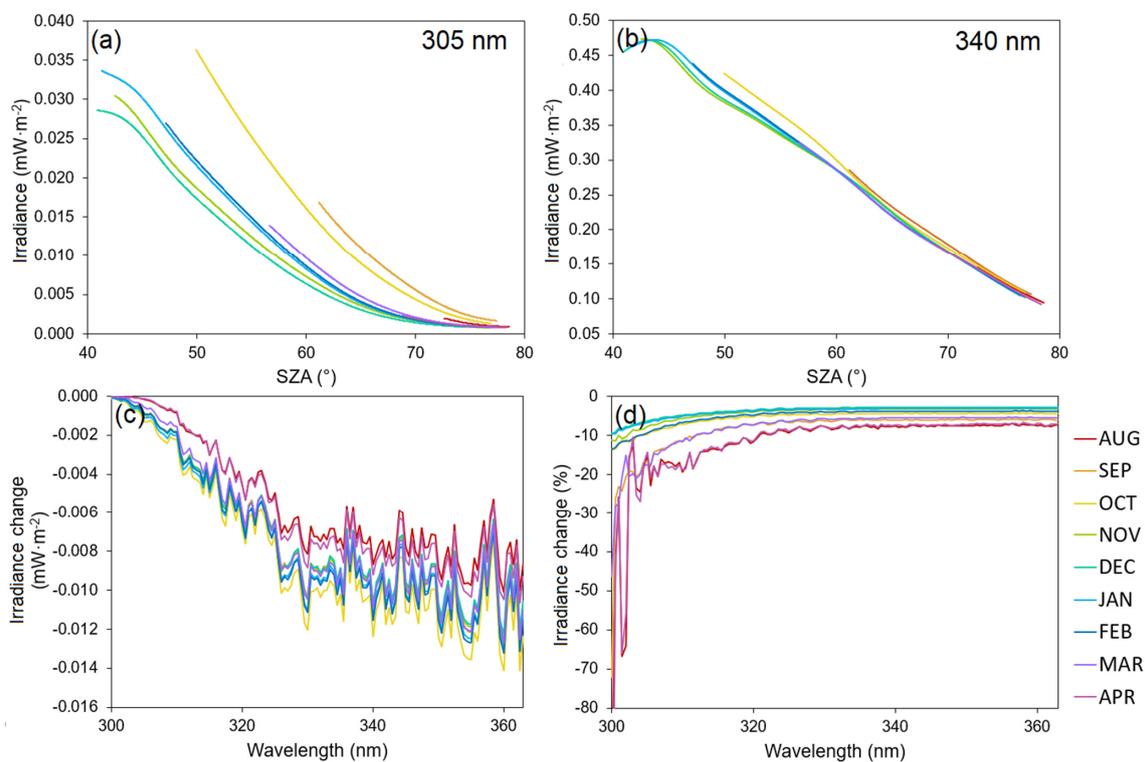
Figure 7: Modelled relationships between UV irradiance and SZA for individual months, and absolute and relative changes in spectral UV irradiance caused by SZA change, while (a) and (b) represent the modelled SZA effect at 305 and 340 nm, respectively, (c) and (d) absolute and relative change in spectral UV irradiance induced by a 1° increase in SZA.

615
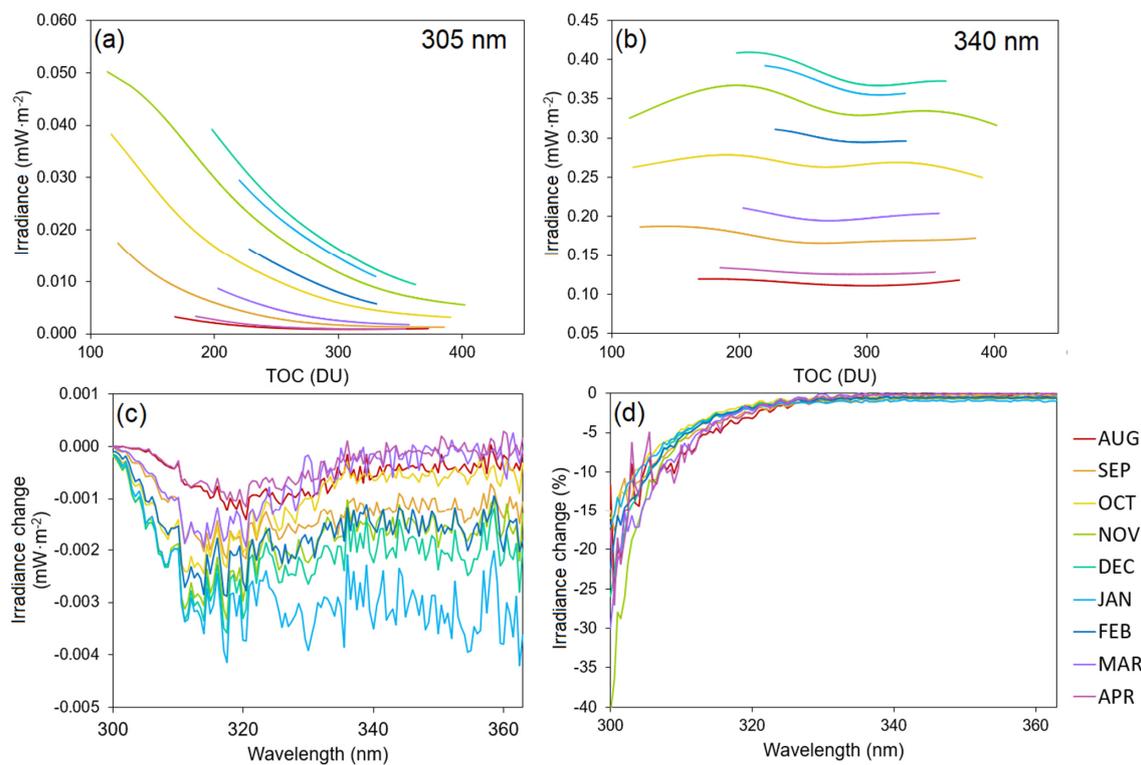
Figure 8: Modelled relationships between UV irradiance and TOC for individual months, and absolute and relative changes in spectral UV irradiance caused by TOC change, while (a) and (b) represent the modelled TOC effect at 305 and 340 nm, respectively, (c) and (d) absolute and relative change in spectral UV irradiance induced by a 10 DU increase in TOC.
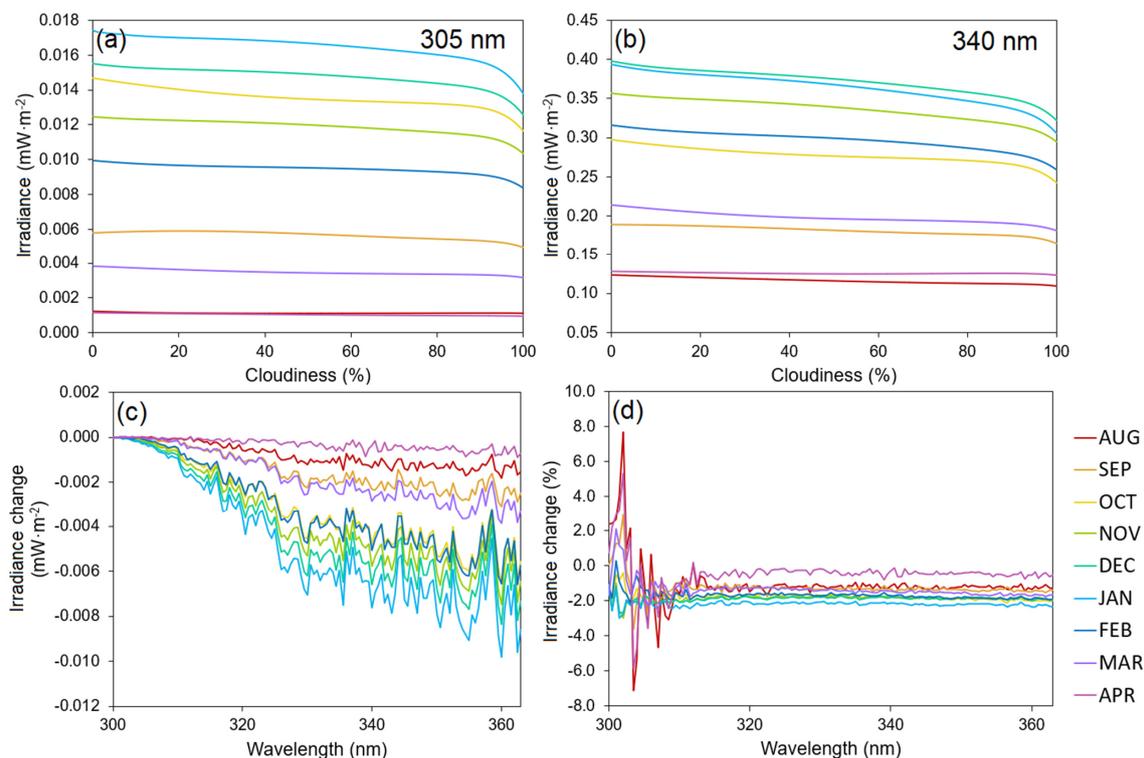
620

Figure 9: Modelled relationships between UV irradiance and cloudiness for individual months, and absolute and relative changes in spectral UV irradiance caused by the change in cloudiness, while (a) and (b) represent the modelled effect of cloudiness at 305 and 340 nm, respectively, (c) and (d) absolute and relative change in spectral UV irradiance induced by a 10 % increase in cloudiness.
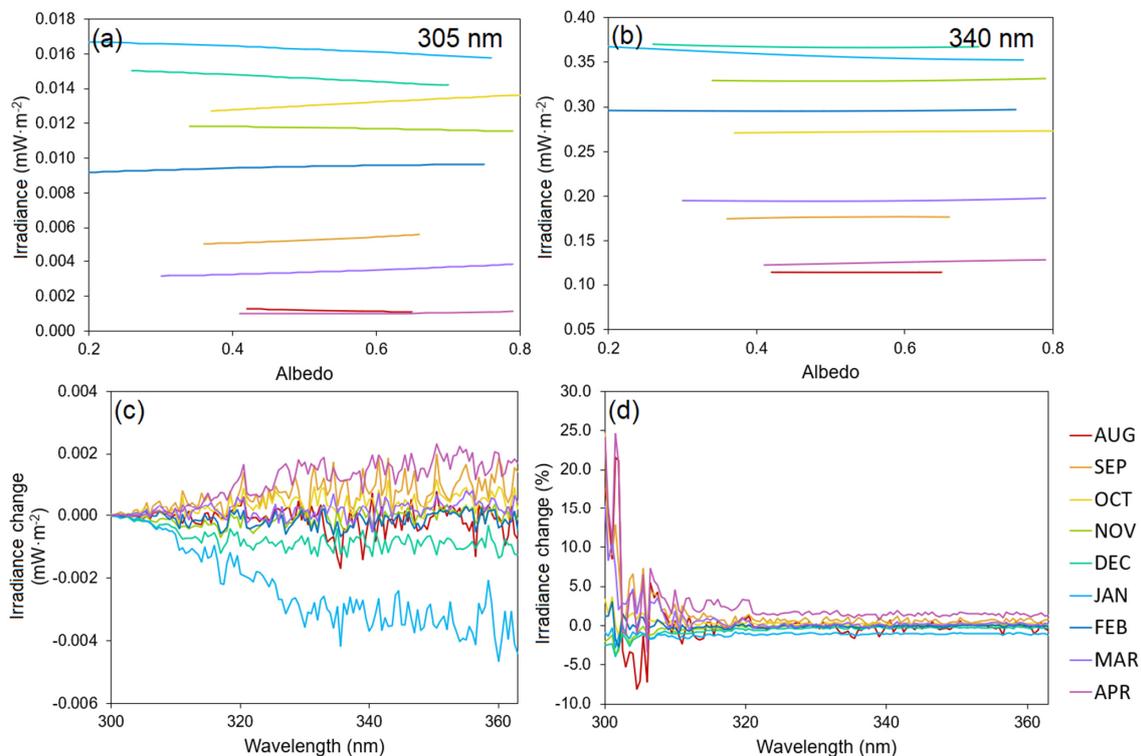
625
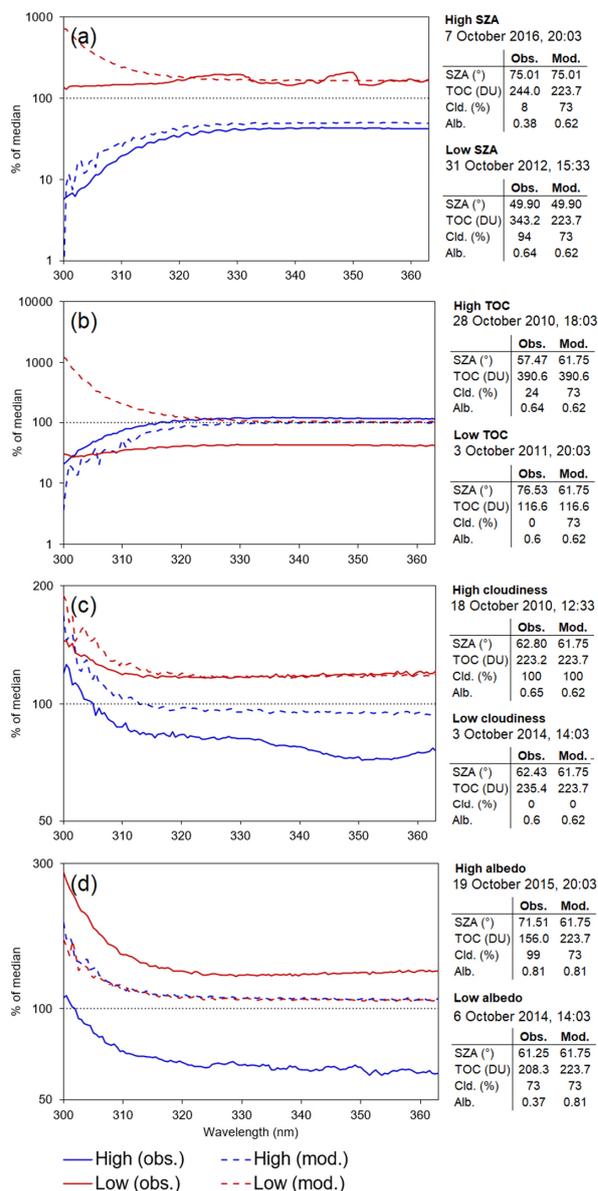
Figure 10: Modelled relationships between UV irradiance and surface albedo for individual months, and absolute and relative changes in spectral UV irradiance caused the change in albedo, while (a) and (b) represent the modelled effect of albedo at 305 and 340 nm, respectively, (c) and (d) absolute and relative change in spectral UV irradiance induced by the increase in albedo by 0.1.

630

High SZA
7 October 2016, 20:03

	Obs.	Mod.
SZA (°)	75.01	75.01
TOC (DU)	244.0	223.7
Cld. (%)	8	73
Alb.	0.38	0.62

Low SZA
31 October 2012, 15:33

	Obs.	Mod.
SZA (°)	49.90	49.90
TOC (DU)	343.2	223.7
Cld. (%)	94	73
Alb.	0.64	0.62

High TOC
28 October 2010, 18:03

	Obs.	Mod.
SZA (°)	57.47	61.75
TOC (DU)	390.6	390.6
Cld. (%)	24	73
Alb.	0.64	0.62

Low TOC
3 October 2011, 20:03

	Obs.	Mod.
SZA (°)	76.53	61.75
TOC (DU)	116.6	116.6
Cld. (%)	0	73
Alb.	0.6	0.62

High cloudiness
18 October 2010, 12:33

	Obs.	Mod.
SZA (°)	62.80	61.75
TOC (DU)	223.2	223.7
Cld. (%)	100	100
Alb.	0.65	0.62

Low cloudiness
3 October 2014, 14:03

	Obs.	Mod.
SZA (°)	62.43	61.75
TOC (DU)	235.4	223.7
Cld. (%)	0	0
Alb.	0.6	0.62

High albedo
19 October 2015, 20:03

	Obs.	Mod.
SZA (°)	71.51	61.75
TOC (DU)	156.0	223.7
Cld. (%)	99	73
Alb.	0.81	0.81

Low albedo
6 October 2014, 14:03

	Obs.	Mod.
SZA (°)	61.25	61.75
TOC (DU)	208.3	223.7
Cld. (%)	73	73
Alb.	0.37	0.81

Legend:
— High (obs.) - - - High (mod.)
— Low (obs.) - - - Low (mod.)

Figure 11: Spectral UV irradiance intensity relative to the monthly median on eight selected October days with extremely high or low (a) SZA, (b) TOC, (c) cloudiness, and (d) albedo at Marambio Base in 2010–2020. The contrast between the model output, where all but one explanatory variables were set to their monthly median, and the actual observation, shows the importance of the other three variables that were set to their medians in the model and whose values are shown in the tables on the right.